

Document downloaded from:

<http://hdl.handle.net/10251/101066>

This paper must be cited as:



The final publication is available at

<http://doi.org/10.1021/acscatal.7b00170>

Copyright American Chemical Society

Additional Information

This document is the Accepted Manuscript version of a Published Work that appeared in final form in

ACS Catalysis, copyright © American Chemical Society after peer review and technical editing by the publisher.

To access the final edited and published work see <http://doi.org/10.1021/acscatal.7b00170>

Nanolayered Co-Mo-S Catalysts for the Chemoselective Hydrogenation of Nitroarenes

*Iván Sorribes, Lichen Liu and Avelino Corma**

Instituto de Tecnología Química, Universitat Politècnica de València-Consejo Superior de Investigaciones Científicas, Avenida de los Naranjos s/n, 46022 Valencia, Spain.

ABSTRACT: Nanolayered molybdenum disulfide cobalt promoted materials (Co-Mo-S) have been established as chemoselective catalysts for the hydrogenation of nitroarenes under relatively mild conditions. Co-Mo-S catalysts have been prepared by a one-pot hydrothermal synthesis that allows for obtaining unsupported catalysts with a high number of active sites per unit volume. Applying these catalysts, the hydrogenation of the nitro functionality has been carried out selectively in the presence of double and triple bonds, aldehydes, ketones as well as carboxylic acid derivatives groups, thus affording the corresponding anilines in good to excellent yields. Interestingly, the partial hydrogenation of some dinitroarenes has also been successfully accomplished. In addition, its catalytic performance has been evaluated for the preparation of the bio-active compound paracetamol through a one-pot direct hydrogenative amidation reaction.

Selective hydrogenation; Nitroarenes; Heterogeneous catalysis; Functionalized anilines; Green hydrogenation chemistry; Nanolayered materials; Co-Mo-S catalysts

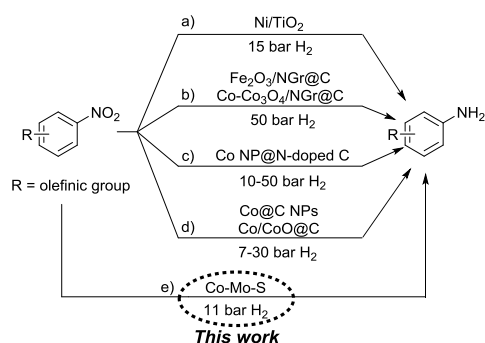
INTRODUCTION

Anilines are important intermediates in the industrial production of agrochemicals, pharmaceuticals, pigments, dyes and polymers.¹ In addition, since they can easily undergo further derivatization reactions, they also represent essential building blocks for the preparation of novel highly-valuable organic compounds at laboratory scale.² Typically, their synthesis involves the introduction of a nitro group into an aromatic compound by nitration, followed by reduction.³ Therefore, it is not surprising that the transformation of nitroarenes into anilines represents one important reaction in organic synthesis that continuously attracts the attention of chemists.

Currently, the environmentally benign commercial production of anilines functionalized with other easily reducible groups, such as unsaturated bonds, remains as an important challenge. In fact, stoichiometric amounts of sodium hydrosulfite,⁴ iron,⁵ tin,⁶ or zinc in ammonia hydroxide⁷ are still being used as reductants to get a preferential selectivity to the nitro group. Among the amenable reduction methodologies, catalytic hydrogenation over heterogeneous catalysts is the preferred choice to substitute these stoichiometric processes.^{3a,8} Traditionally, noble metal-based heterogeneous catalysts are by far the most widespread materials used for the chemoselective hydrogenation of nitroarenes.⁹ For instance, Blaser *et al.* reached chemoselectivity by applying commercially available Pt supported catalysts modified with Pb or H₃PO₄, but additional amounts of iron and vanadium salts in solution were required respectively to avoid the accumulation of partially reduced intermediates.¹⁰ Later on, by tailoring the particle size and controlling the metal-support interactions, we developed heterogeneous chemoselective catalysts based on gold,¹¹ platinum and ruthenium^{11e,11f,12} with an optimal and broad-spectrum

performance. Our work was followed by others¹³ that expanded the catalysts available to other metals such as silver¹⁴ and rhodium.¹⁵

However, the high price and limited availability of these precious metals prevent their large scale application, and therefore there exists a strong initiative to design heterogeneous catalysts based on earth-abundant metals for the chemoselective hydrogenation of nitroarenes.^{8b} Nonetheless, only a scarce number of cost-effective catalysts that can selectively hydrogenate nitro compounds in the presence of olefinic bonds have so far been described (Scheme 1).



Scheme 1. Hydrogenation of nitroarenes functionalized with C=C double bonds over non-precious metal-based heterogeneous catalysts

In 2008, our group developed a TiO₂-supported Ni-based catalyst able to carry out this chemoselective hydrogenation under mild conditions (15 bar H₂; Scheme 1a).^{12a} Later, Beller *et al.* reported the hydrogenation of nitroarenes under considerably higher pressure conditions (50 bar H₂) by applying cobalt- or iron-based carbon supported catalysts (Co-Co₃O₄/NGr@C or Fe₂O₃/NGr@C), in which nanoparticles are encapsulated by a nitrogen-enriched graphene-layer matrix (Scheme 1b).¹⁶ Recently, their catalytic activity has been improved, but equimolecular amounts of base in solution are required.¹⁷ Lately, other catalysts based on cobalt nanoparticles supported on nitrogen-doped carbon matrix have been also applied for the hydrogenation of

nitroarenes achieving a remarkable selectivity although they also work under high hydrogen pressures (Scheme 1c).¹⁸ It should be noticed that for all of these nanostructured metals modified by N-doped carbon supports, the presence of nitrogen has been established crucial for the catalytic performance of these systems. Interestingly, quite recently we have demonstrated that the hydrogenation of nitroarenes can be conducted selectively on nitrogen-free Co@C nanoparticles under much milder conditions (7 bar H₂; Scheme 1d).¹⁹

Dinuclear and trinuclear molybdenum (IV) complexes containing bridging sulfide ligands have been proposed as efficient homogeneous catalysts for the preparation of functionalized anilines from the corresponding nitroarenes in the presence of different reducing agents, such as, hydrogen, formates or hydrosilanes.²⁰ Commercial MoS₂ and an oxygen-implanted MoS₂ catalyst can also efficiently catalyze this transformation by transfer hydrogenation using hydrazine as the hydrogen source.²¹ However, to the best of our knowledge, the use of molybdenum sulfide-type heterogeneous catalysts for the more benign hydrogenation of nitroarenes is scarce. There exists only few examples in which the non-functionalized aniline has been achieved in low yield (<40 %) or under harsh conditions (<300 °C and/or up to 40 bar H₂) by using MoS₂,²² Zr-intercalated MoS₂,²³ or the Chevrel phases²⁴ as catalysts in the presence of hydrogen.

Herein, we show the synthesis of nanolayered molybdenum disulfide cobalt promoted materials (Co-Mo-S) by a one-pot hydrothermal synthesis. These unsupported materials with a high number of active sites per unit volume are able to carry out the chemoselective hydrogenation of substituted nitroarenes under mild reaction conditions (Scheme 1e). Based on their catalytic behavior, we also show that these nanolayered Co-Mo-S catalysts allow carrying out the synthesis of paracetamol through a one-pot direct hydrogenative amidation reaction.

RESULTS AND DISCUSSION

Catalysts Preparation and Characterization

Molybdenum sulfide bulk materials has been described as a layered structure wherein the covalent bonded S-Mo-S trilayers are weakly held together by van der Waals interactions.^{22,25} Interestingly, active sites of these catalysts are supposed to be located on the edges of the sandwich S-Mo-S layers, which can absorb cobalt as promoter leading to a Co-Mo-S phase and thereby increasing considerably their catalytic activity.²⁶ This promotional effect has been attributed to a lower binding energy of cobalt relative to that of molybdenum with sulfur at the edges of MoS₂, thus making easier the generation of vacant active sites.²⁷ Additionally to these coordinatively unsaturated sites, the “brim” of the edges with metal-like electronic states has also been established as potentially active sites able to activate different organic molecules.^{26,26o,28}

For decades, tremendous efforts have been made worldwide to enhance the activity of metal sulfide catalysts. Since the development of the so-called NEBULA catalyst,²⁹ which include a higher population of active sites per unit volume, unsupported metal sulfides have emerged as a convenient alternative for conventional supported catalysts.³⁰ In this respect, different methodologies have been developed for the preparation of unsupported sulfide catalysts.³¹ Among them, the hydrothermal synthesis represents the most potential process for producing highly homogeneous materials and for controlling their morphology.^{30a,32}

Based on this background, we attempted the preparation of an active MoS₂-based catalyst able to catalyze the hydrogenation of nitroarenes under relatively mild conditions by exploring the preparation of unsupported Co-Mo sulfide catalysts by a one-pot hydrothermal method. More specifically, ammonium molybdate as the Mo source, sulfur powder and variable amounts of

cobalt (II) acetate were reacted at different temperatures in the presence of an aqueous solution of hydrazine. The resultant nanolayered catalysts were denoted as Co-Mo-S-X-T, where X and T represent the Co/(Mo+Co) mole ratio in the final catalyst determined by ICP analysis and the temperature used in its preparation, respectively. For comparison, the cobalt-free molybdenum disulfide material was also synthesized by using the same preparation methodology (see experimental section for details on the preparation).³³

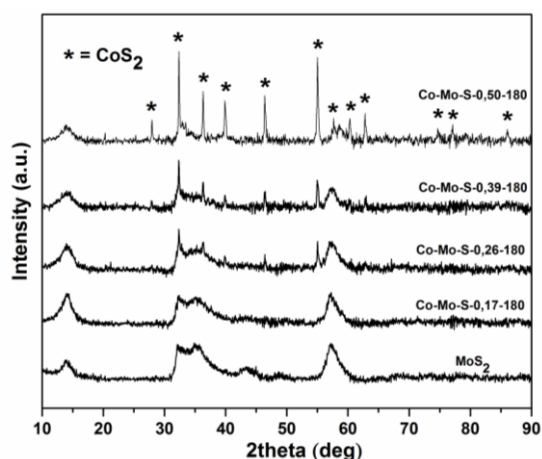


Figure 1. XRD patterns of nanolayered catalysts MoS₂ and Co-Mo-S with different cobalt contents

Figure 1 shows the XRD patterns of a series of catalysts prepared at the same temperature (180 °C) with increasing amounts of cobalt. All of them exhibit some broad diffraction peaks at $2\theta = 14^\circ, 33^\circ, 36^\circ, 59^\circ$ corresponding to the (002), (100), (103) and (110) basal planes of the poorly crystalline hexagonal structure of MoS₂ (PDF code 96-101-0994). In addition, some other diffraction peaks that match well with CoS₂ (PDF code 00-041-1471) become noticeable and sharper progressively by increasing the cobalt loading. The absence of these peaks in the catalyst prepared with lower amount of cobalt (Co-Mo-S-0.17-180) indicates that CoS₂ is highly

dispersed on MoS₂ and/or as very small particles.^{32c} In general, XRD picks of the ternary Co-Mo-S phase are not detected, probably owing to its overlapping with diffraction picks of MoS₂, or because this phase exists as very small nano-crystallites.^{27,32a}

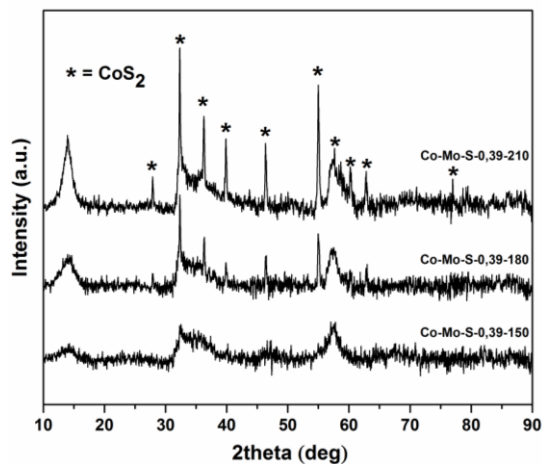


Figure 2. XRD patterns of nanolayered catalysts Co-Mo-S-0.39 prepared at different temperature

The effect of the temperature in the catalyst preparation was also studied. As shown Figure 2, XRD patterns of the amorphous Co-Mo-S-0.39-T (T = 150, 180 and 210 °C) catalysts present significant differences, meaning that temperature has a high impact on the crystal structure. At 150 °C the XRD pattern is characteristic of a poorly crystallized MoS₂-like phase with no obvious formation of CoS₂. However, the CoS₂ phase becomes perceptible with the increase of temperature, suggesting the progressive formation of separated CoS₂ in large particle size on the surface of the catalyst. It is noteworthy that the (002) peak, associated with the stacking of the atomic layers, undergoes a significant increase with the temperature.

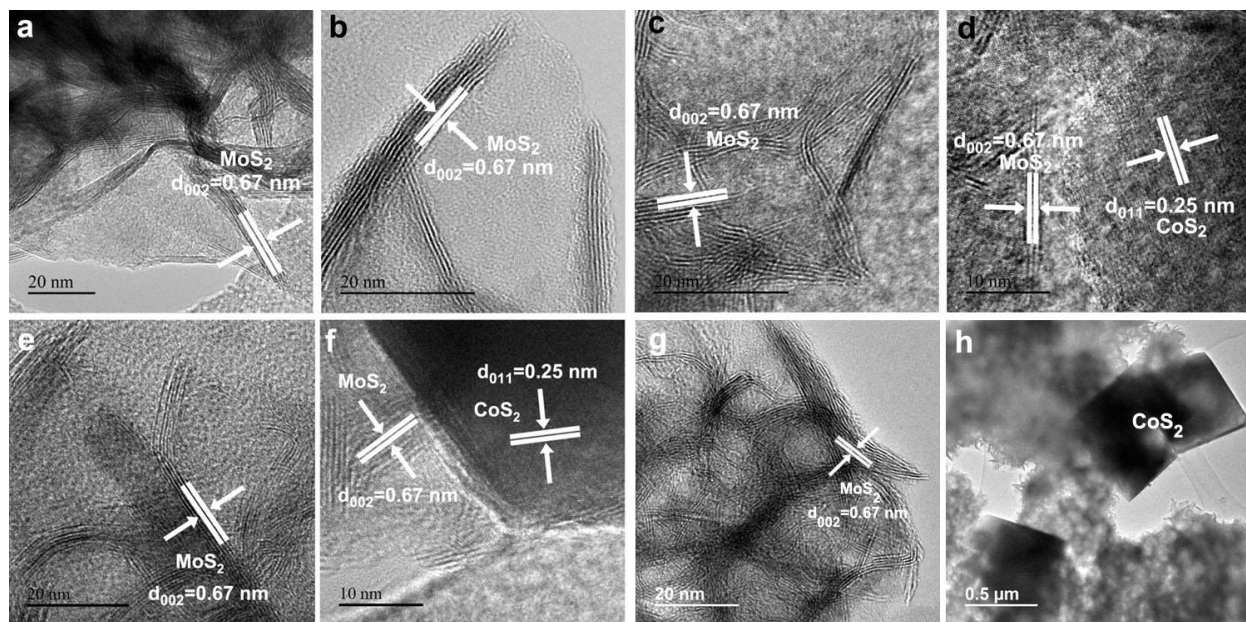


Figure 3. HRTEM images of MoS₂ (a), Co-Mo-S-0.17-180 (b), Co-Mo-S-0.26-180 (c-d), Co-Mo-S-0.39-180 (e-f) and Co-Mo-S-0.50-180 (g-h)

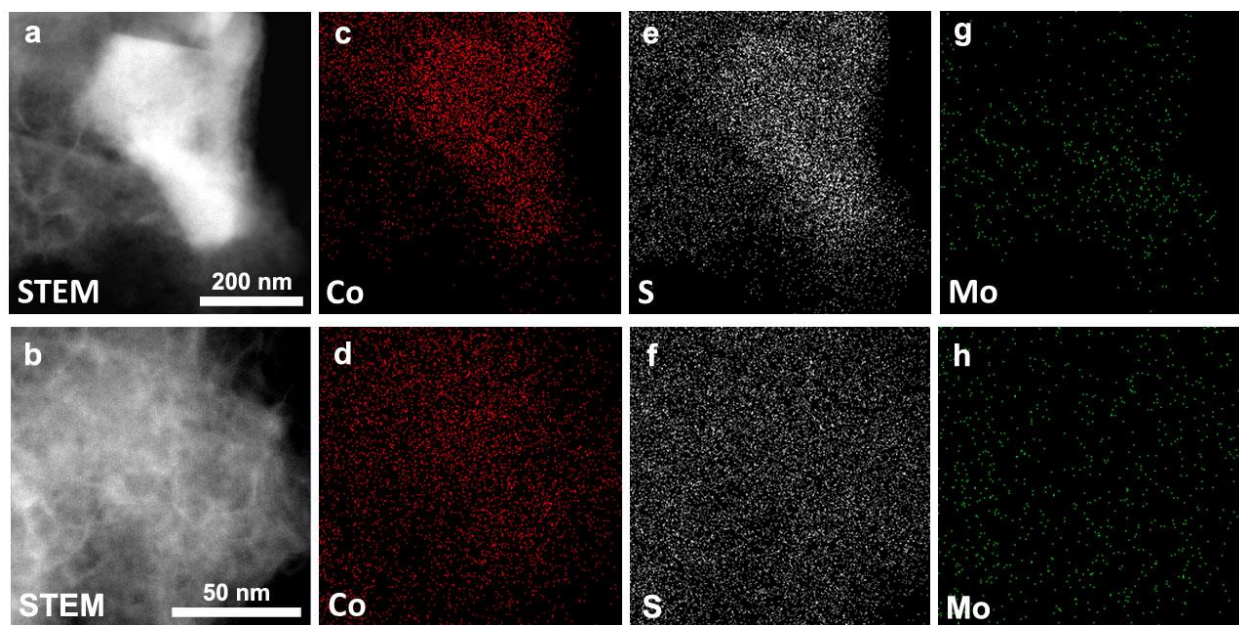


Figure 4. STEM-HAADF images of Co-Mo-S-0.39-180 (a, b). Elemental mapping of sulfur, cobalt, and molybdenum (c-h)

The micro-structure and elemental distributions of the nanolayered MoS₂ and Co-Mo-S catalysts prepared at 180 °C with different Co/(Mo+Co) mole ratio were investigated by electron microscopy. As shown Figure 3, all catalysts display the typical parallel black thread-like fringes with an interlayer distance of 0.65 nm, which is characteristic of the (002) basal planes of the hexagonal MoS₂ structure.³⁴ It should be note that no clear differences in the slab and stack size distribution (ca. 50 and 5 nm, respectively) of these black thread-like fringes have been observed with the increase of cobalt loading. Notably, no other fringes are detected in catalyst Co-Mo-S-0.17-180 (Figure 3b) because cobalt is highly dispersed on the catalyst surface, as reveals the XEDS elemental mapping (Figure S1 in the Supporting Information). However, in the HRTEM images of catalysts with higher cobalt loading a separated CoS₂ phase can also be detected in the form of large nanoparticles with a wide range of size distributions (Table S1 in the Supporting Information) that present the characteristic spacing of 0.25 nm of its lattice fringes (Figure 3c-h). In concordance with XRD results, this separated CoS₂ phase becomes more evidenced with the increase of cobalt loading in the catalyst. Nevertheless, a homogeneous distribution of cobalt on the lamellar structure of MoS₂ can still be observed in all catalysts by XEDS elemental mapping (Figure 4 and Figures S2 and S3 in the Supporting Information).

Textural parameters of the catalysts prepared at 180 °C are listed in Table 1. Cobalt-free MoS₂ catalyst presents a surface area and pore volume of 50.6 m²/g and 0.06 cm³/g, respectively. They are smaller than for related materials previously reported, as consequence of the use of different preparation methods.^{30a,32c} Under hydrothermal conditions the particle agglomeration is produced in some extent, thus leading to a lower surface area of the resulting materials.^{32f} Interestingly, by increasing the cobalt loading, both surface area and pore volume first decrease to 8.1 m²/g and 0.02 cm³/g in catalyst Co-Mo-S-0.17-180, and then increase up to 74.0 m²/g and 0.17 cm³/g with

the highest cobalt containing catalyst (Co-Mo-S-0.50-180), respectively. This behavior in the textural parameters upon addition of a metal promoter (Co or Ni) has already been reported for other related materials.^{32j,35} The first decreasing on surface area and pore volume in catalyst Co-Mo-S-0.17-180 is ascribed to the blockage of the pore channels of MoS₂. However, in catalysts with higher cobalt loading the CoS₂ phase, which has been inferred from XRD and TEM results, can also act as a support for MoS₂ and the presumed generated Co-Mo-S phase, thus increasing considerably the surface area and pore volume of the catalysts.

Table 1. Textural parameters of MoS₂ and Co-Mo-S catalysts synthesized at 180 °C

| Catalyst | Surface Area (m ² /g) | Pore Volume (cm ³ /g) | Pore Diameter (nm) |
|------------------|-------------------------------------|-------------------------------------|-----------------------|
| MoS ₂ | 50.6 | 0.06 | 6.8 |
| Co-Mo-S-0.17-180 | 8.1 | 0.02 | 15.4 |
| Co-Mo-S-0.26-180 | 24.9 | 0.06 | 10.8 |
| Co-Mo-S-0.39-180 | 71.4 | 0.16 | 9.2 |
| Co-Mo-S-0.50-180 | 74.0 | 0.17 | 9.7 |

Catalytic Results

As we highlighted above, chemoselectivity is crucial for the current applicability of heterogeneous catalysts in nitroarenes hydrogenation. Therefore, 3-nitrostyrene (**1a**) was selected as a model substrate because the nitro group is accompanied by one of the most easily reducible functionalities, i.e. an olefinic group. Initial hydrogenation experiments, focused on the identification of the most active nanolayered Co-Mo-S catalyst, were conducted under relatively mild conditions (11 bar of H₂, 150 °C) and using toluene as solvent. Previous experiments using only toluene as reactant, showed no hydrogenation activity under our reaction conditions. As shown Figure 5a, the use of cobalt as promoter in the catalyst preparation has a significant effect

in their catalytic activity. Indeed, an enhanced conversion of **1a** is achieved by increasing the cobalt loading up to a Co/(Mo+Co) mole ratio of 0.39, as result of the formation of more active sites with the progressive addition of cobalt.^{32a} Interestingly, under otherwise the same reaction conditions the Co-Mo-S-0.39-180 catalyst displays a slightly higher activity (measured by the initial reaction rates normalized to the mass of metal weight) than the recently reported nitrogen-free Co@C nanoparticles.^{19a} However, a further increase of this ratio leads to detrimental results that could be associated to the over-formation of the separated CoS₂ phase, as it has been inferred from XRD and TEM characterization (see Figure 1 and 3, respectively). Indeed, only a negligible conversion of **1a** was achieved by using CoS₂ as catalyst (Table 2, entry 1).

Likewise, since catalyst preparation temperature affects to the phase composition of the resulting materials (see Figure 2), an important impact on their catalytic activity should be also expected. As shown Figure 5b, the catalytic activity increase when the catalyst preparation temperature is augmented from 150 °C to 180 °C. Nevertheless, **1a** undergoes a lower conversion in the presence of the catalyst prepared at 210 °C (Co-Mo-S-0.39-210), temperature for which the separated CoS₂ phase is produced in larger extent.

To further investigate the role of the separated CoS₂ phase in the hydrogenation of nitroarenes catalyzed by the nanolayered Co-Mo-S catalysts, some control experiments were carried out on the model substrate **1a**. For this purpose, two additional catalysts with the same Co/(Mo+Co) mole ratio (0.21) were prepared, one by a two-step hydrothermal method (MoS₂-CoS₂-0.21-180; see Figures S4 and S5 in the Supporting Information), and the other one physically mixing separately prepared MoS₂ and CoS₂ (MoS₂+CoS₂-0.21). It should be note that while some ternary Co-Mo-S phase can be formed by the two-step hydrothermal method, it must be excluded in the mechanical mixture. Even so, if the promotional influence of cobalt results from a

synergetic contact effect between MoS₂ and CoS₂ phases, both catalysts should present a similar catalytic activity. However, when **1a** was submitted to the optimized conditions in the presence of catalyst MoS₂-CoS₂-0.21-180, a moderate yield of 3-vinylaniline (**2a**) was afforded (59%; Table 2, entry 3). Meanwhile, only 16% yield of **2a** was obtained with catalyst MoS₂+CoS₂-0.21 (Table 2, entry 4), which can be ascribed to the activity of the separated phases of MoS₂ and CoS₂. Therefore, in agreement with the Edge Decoration model proposed by Topsøe *et al.*,^{26a-c,26e,26l} the high activity of the prepared nanolayered catalysts for the hydrogenation of nitroarenes can be attributed to the formation of Co-Mo-S active structures rather than to a synergistic effect between MoS₂ and CoS₂ phases.³⁶

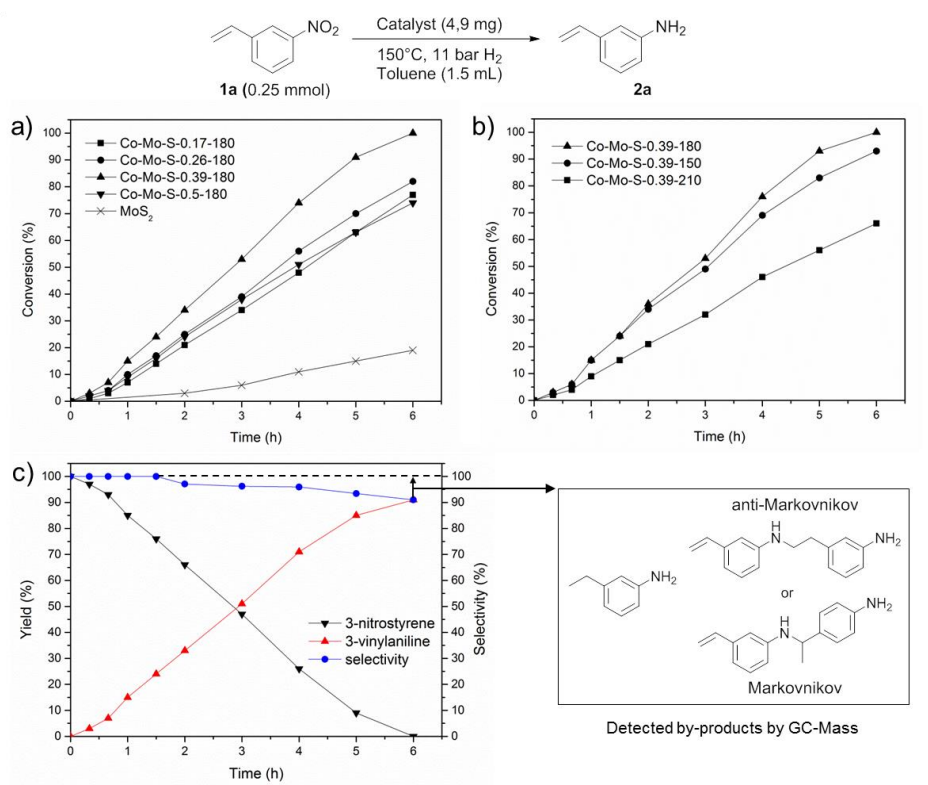
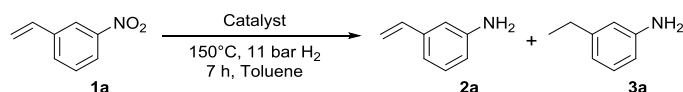


Figure 5. Catalytic performance for the hydrogenation of 3-nitrostyrene (1a**) to 3-vinylaniline (**2a**) in the presence of: a) nanolayered catalysts with different cobalt content; b) Co-Mo-S-0.39 catalysts prepared at different temperature. c) Concentration/time**

diagram and selectivity for catalyst Co-Mo-S-0.39-180. The inset shows the by-products detected by GC-Mass

Table 2. Co-Mo-S catalyzed hydrogenation of 3-nitrostyrene (1a)^a



| Entry | Catalyst | Conv. (%) ^b | Yield (%) ^b | |
|-------------------|--|------------------------|------------------------|-----------|
| | | | 2a | 3a |
| 1 | CoS ₂ | 21 | 19 | - |
| 2 | MoS ₂ | 20 | 17 | - |
| 3 | MoS ₂ -CoS ₂ -0.21-180 | 65 | 59 | 4 |
| 4 | MoS ₂ +CoS ₂ -0.21 | 20 | 16 | - |
| 5 | Co-Mo-S-0.17-180 | 79 | 74 | 2 |
| 6 | Co-Mo-S-0.26-180 | 83 | 77 | 2 |
| 7 | Co-Mo-S-0.39-180 | >99 | 91 (83) | 3 |
| 8 | Co-Mo-S-0.5-180 | 75 | 71 | 1 |
| 9 | Co-Mo-S-0.39-150 | 95 | 88 | 5 |
| 10 | Co-Mo-S-0.39-210 | 69 | 63 | 1 |
| 11 ^c | Co-Mo-S-0.39-180 | 94 | 89 | 2 |
| 12 ^{c,d} | Co-Mo-S-0.39-180 | 84 | 82 | - |
| 13 ^{c,e} | Co-Mo-S-0.39-180 | 90 | 85 | 3 |
| 14 ^f | Co-Mo-S-0.39-180 | 79 | 74 | 1 |
| 15 ^g | Co-Mo-S-0.39-180 | 60 | 55 | - |

^aReaction conditions: **1a** (0.25 mmol), catalyst (4.9 mg), toluene (1.5 mL). ^bDetermined by GC using dodecane as an internal standard; yield of isolated product in parentheses. ^c6 h. ^dMeOH as solvent. ^eEtOH as solvent. ^f120 °C, 21 h. ^g6 bar H₂

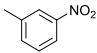
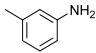
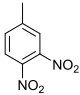
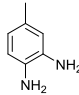
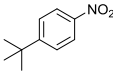
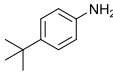
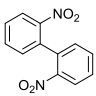
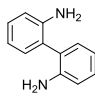
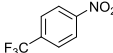
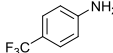
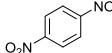
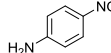
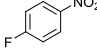
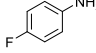
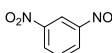
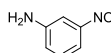
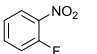
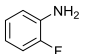
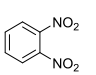
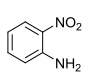
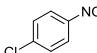
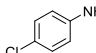
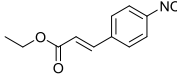
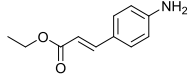
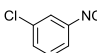
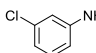
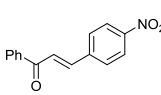
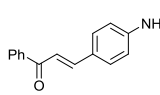
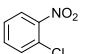
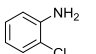
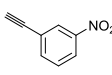
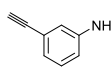
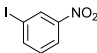
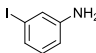
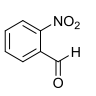
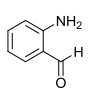
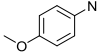
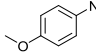
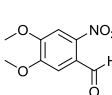
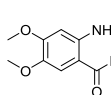
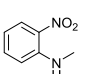
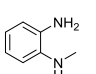
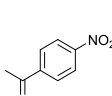
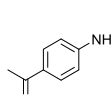
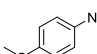
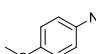
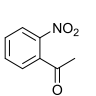
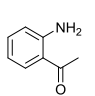
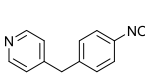
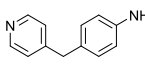
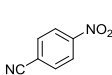
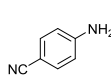
With respect to selectivity, as shown Figure 5c, the most active catalyst (Co-Mo-S-0.39-180) displays a good chemoselectivity toward the hydrogenation of the nitro group affording 3-vinylaniline (**2a**) in 91% yield after full conversion with only residual amounts of 3-ethylaniline (**3a**) (Table 2, entry 7). Traces of a second by-product, generated by the auto-hydroamination of **2a**, were also detected by GC-Mass analysis (see inset of Figure 5c). It should be noted that

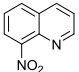
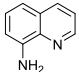
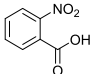
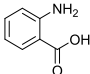
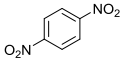
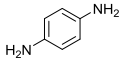
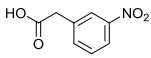
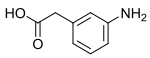
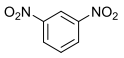
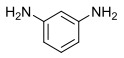
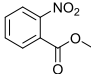
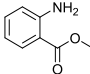
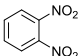
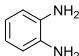
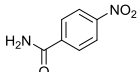
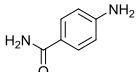
selectivity gradually decreases for longer reaction times because of the unavoidable polymerization of **2a**, and to a lesser extent to the formation of **3a**. (Figure S6 in the Supporting Information). Interestingly, high chemoselectivity is achieved in all prepared materials, being their catalytic differences mainly on activity (Table 2, entries 5-10; see also Figure S6 in the Supporting Information). It is well-established that the way in which the substituted nitroarene is adsorbed on the catalyst surface determines the degree of selectivity.^{11c,19a} Since CoS₂ and the non-promoted MoS₂ catalysts also display a high chemoselectivity in the hydrogenation of **1a** (Table 2, entries 1-2), the electronic effects generated because of the presence of cobalt as promoter should be disregarded as the main cause of the selectivity. So, the presence of metal-sulfur bonds appears to have a key role on the preferential adsorption through the nitro group.

The use of different solvents in the presence of catalyst Co-Mo-S-0.39-180 was also investigated (Table S2 in the Supporting Information). Excellent conversions and selectivities were reached with protic solvents such as methanol and ethanol, but toluene remained as the best tested solvent (Table 2, entries 11-13). Interestingly, H₂-D₂ exchange experiments (Figure S7 in the Supporting Information) reveals that catalyst is able to activate the H₂ molecule at 120 °C. Indeed, a moderate yield of **2a** was obtained at this temperature or at lower hydrogen pressure (6 bar) by increasing the reaction time (Table 2, entries 14 and 15, respectively).

Table 3. Co-Mo-S catalyzed hydrogenation of different nitroarenes.^a

| Entry | Substrate | Product | Conv. (%) ^b | Yield (%) ^b | Entry | Substrate | Product | Conv. (%) ^b | Yield (%) ^b |
|----------------|-----------|---------|------------------------|------------------------|-------------------|-----------|---------|------------------------|------------------------|
| 1 ^c | | | >99 | >99 (95) | 19 ^{g,e} | | | >99 | (90) |

| | | | | | | | | | |
|-----------------|---|---|-----|-------------|---------------------|--|---|-----|-------------|
| 2 |  |  | >99 | >99 (91) | 20 ^{g,i} |  |  | >99 | (90) |
| 3 |  |  | >99 | >99 (95) | 21 ^{g,h} |  |  | >99 | (94) |
| 4 |  |  | >99 | >99 (92) | 22 |  |  | >99 | 90 (83) |
| 5 |  |  | >99 | >99 (87) | 23 |  |  | 96 | 86 (81) |
| 6 |  |  | >99 | >99 (85) | 24 ⁱ |  |  | 98 | 89 (81) |
| 7 ^d |  |  | >99 | 99 (90) | 25 |  |  | >99 | (94) |
| 8 |  |  | >99 | >99 (96) | 26 |  |  | >99 | (93) |
| 9 |  |  | >99 | 99 (88) | 27 ^{i,j} |  |  | >99 | 80 (69) |
| 10 |  |  | >99 | 96 (91) | 28 ^{f,j,k} |  |  | >99 | 95 |
| 11 |  |  | >99 | >99 (94) | 29 ^{f,j,k} |  |  | >99 | (90) |
| 12 |  |  | >99 | >99 (92) | 30 |  |  | >99 | 99 (91) |
| 13 |  |  | >99 | 89 (80) | 31 |  |  | >99 | 96 (86) |
| 14 ^e |  |  | >99 | (94) | 32 ^h |  |  | >99 | >99 (92) |

| | | | | | | | | | |
|-------------------|---|---|-----|------------|-----------------|--|---|-----|-------------|
| 15 ^f |  |  | >99 | 97 (90) | 33 ^h |  |  | >99 | (90) |
| 16 ^{g,h} |  |  | >99 | (85) | 34 ^h |  |  | >99 | (91) |
| 17 ^{g,e} |  |  | >99 | (95) | 35 |  |  | >99 | >99 (95) |
| 18 ^{g,i} |  |  | >99 | (89) | 36 ^f |  |  | >99 | 99 (93) |

^aReaction conditions: substrate (0.25 mmol), catalyst (4.9 mg), toluene (1.5 mL). ^bDetermined by GC using dodecane as an internal standard; yield of isolated product in parentheses. ^cConversion and yield determined using hexadecane as an internal standard; yield of isolated product on 10 mmol scale. ^d14 h, 120 °C. ^e10 h. ^f15 h. ^gCatalyst (9.8 mg). ^h8 h. ⁱ12 h. ^jPlease, see Extension of Table 3 in the Supporting Information. ^k30 bar H₂, 120 °C.

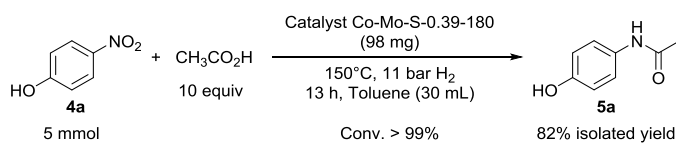
The scope of catalyst Co-Mo-S-0.39-180 was evaluated in the hydrogenation of a wide range of nitroarenes containing diverse substituents groups (Table 3). Simple nitrobenzene, alkyl- and trifluoromethyl-substituted nitroarenes are smoothly hydrogenated giving quantitative yields (Table 3, entries 1-4). Halide-containing anilines are obtained in up to 99% yield by hydrogenation of the corresponding nitro compounds, albeit a lower temperature (120 °C) was used for 4-chloronitrobenzene to avoid dehalogenation (<3% at 150 °C) (Table 3, entries 5-10). The electron-donating methoxy- and *N*-methylated groups are also well tolerated affording the corresponding anilines in quantitative yields (Table 3, entries 11-12). Likewise, *N*-heterocyclic nitro compounds are full converted at longer reaction times giving excellent yields of the respective amino-substituted *N*-heterocycles (Table 3, entries 14-15). However, a slightly lower yield (89 %) is achieved for 4-(methylthio)aniline because a hydrodesulfurization (HDS) reaction is produced in some extent (Table 3, entry 13).

Aromatic diamines are of industrial interest as monomers for the synthesis of multifunctional polymers.³⁷ So, the hydrogenation of different dinitro compounds was investigated. Pleasingly, by using a higher catalyst loading these substrates were successfully hydrogenated to the diamines in good to excellent yields (Table 3, entries 16-21). The partial hydrogenation of these dinitroaromatics was also attempted, and for non-substituted dinitrobenzene compounds, the corresponding nitroanilines are achieved in high yields independently of the nitro groups ring position (Table 3, entries 22-24). To the best of our knowledge, this partial hydrogenation remains elusive in the presence of heterogeneous catalysts. A reaction profile of the hydrogenation of 1,4-dinitrobenzene in the presence of catalyst Co-Mo-S-0.39-180 reveals its lower reactivity compared with the partially hydrogenated 4-nitroaniline, thus suggesting that this selectivity is associated with a preferential adsorption of the dinitro compounds on the catalyst surface (Figure S8 in the Supporting Information).

To further investigate the chemoselectivity of the nanolayered catalyst Co-Mo-S-0.39-180, some additional substrates containing other easily reducible moieties were also tested. Apart from the benchmark substrate, **1a**, two olefinic nitro compounds were processed under optimized reaction conditions. In both cases, double bonds are retained obtaining the corresponding anilines in excellent yields, and only traces (<2%) of products with reduced C=C double bond (Table 3, entries 25-26) were detected. The alkyne group of 1-ethynyl-3-nitrobenzene is also well tolerated and the hydrogenated 3-ethynylaniline is obtained in 80% yield (Table 3, entry 27; see also Scheme S1 in the Supporting Information). Hydrogenation of the nitro group is susceptible to the presence of aldehyde functionalities. Even so, by using an increased pressure (30 bar H₂) excellent yields of the aldehyde-substituted anilines are achieved (Table 3, entries 28-29; for experimental details, see Section SI6 in the Supporting Information). Interestingly, substrates

containing keto substituents in different ring position are also smoothly converted into the corresponding amines in up to 99% yield (Table 3, entries 30-31). Moreover, carboxylic acid derivatives, such as cyanide, acids, esters and amides, are also suitable groups to be present in the selective hydrogenation of the nitro functionality because they remain totally unaffected, thus furnishing the expected anilines in excellent yields (Table 3, entries 32-36).

It should be noted that no traces of reaction intermediates, such as the azoxy-, azo-, hydrazo- or hydroxylamine derivatives were detected. However, hydrogenation of these reaction intermediates affords the expected aniline in nearly quantitative yield, thus suggesting that both generally accepted reaction routes, the direct or the dimerization pathway,³⁸ are feasible for this catalytic system (Scheme S2 and Table S3 in the Supporting Information).



Scheme 2. Catalytic synthesis of paracetamol by a one-pot hydrogenative amidation of *p*-nitrophenol with acetic acid

On the bases of the good hydrogenation reactivity of the nanolayered molybdenum disulfide cobalt promoted material Co-Mo-S-0.39-180, we thought that this could be a good catalyst for the synthesis of paracetamol (N-acetyl-*p*-aminophenol, acetaminophen) through a one-pot hydrogenative amidation reaction. As shown Scheme 2, paracetamol has been isolated in 82% yield by reaction of *p*-nitrophenol with acetic acid in the presence of molecular hydrogen. Many commercial routes have been explored for paracetamol production, and some of them involve the reduction of *p*-nitrophenol, followed by N-acetylation in two separated individual stages.³⁹ In

principle, the one-pot direct amidation reaction might allow for a more benign and practical approach for the synthesis of paracetamol since the isolation of the amine intermediate is avoided. However, the direct acetamidation reaction of *p*-nitrophenol has been scarcely investigated. So far, paracetamol has been prepared in 60% yield through a thiocyanate-mediated one-step reaction.⁴⁰ In addition, catalytic systems, such as Pt nanowires/H₂⁴¹ or Co complexes/silanes,⁴² have been also applied for the direct reductive amidation with acetic acid affording paracetamol in 82 and 85% yield, respectively. Interestingly, our catalytic sequence offers compelling advantages since it avoids different drawbacks of these protocols, i.e. the use of noble metals, low atom-efficiency or laborious workup procedures.

The catalyst recyclability was explored by using 3-nitrostyrene (**1a**) and nitrobenzene as substrates. The nanolayered catalyst Co-Mo-S-0.39-180 was reused five and seven times, respectively, without any reactivation (Figure 6 and Figure S9 in the supporting Information). In both cases, catalytic activity is gradually decreased, although excellent yields and selectivities are obtained after prolonged reaction times.

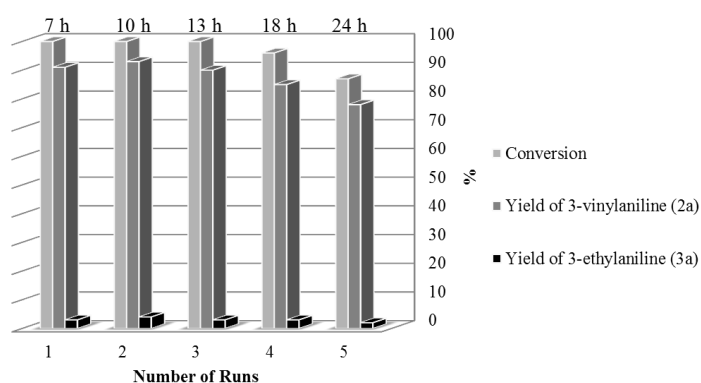


Figure 6. Catalyst recycling for the hydrogenation of 3-nitrostyrene (1a**). Please, see Table 3 for reaction conditions**

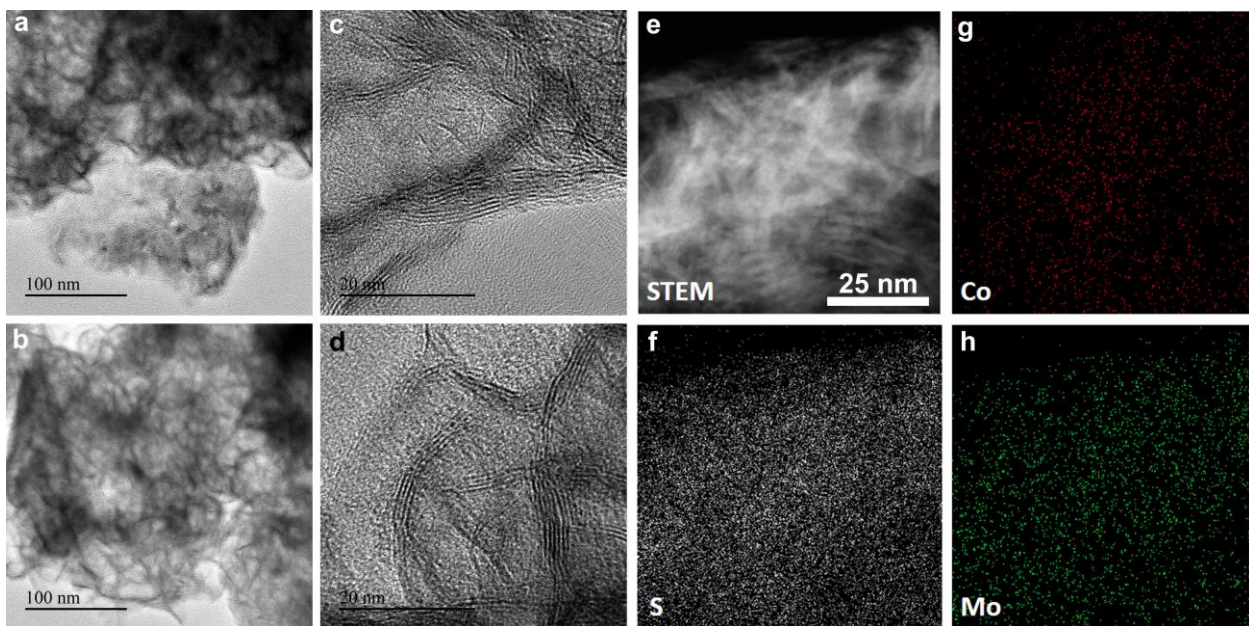


Figure 7. Morphological characterization of Co-Mo-S-0.39-180-R1 in two different areas. Low-magnification TEM images (a-b). HRTEM images (c-d). STEM-HAADF image (e). Elemental mapping of sulfur, cobalt and molybdenum (f-h)

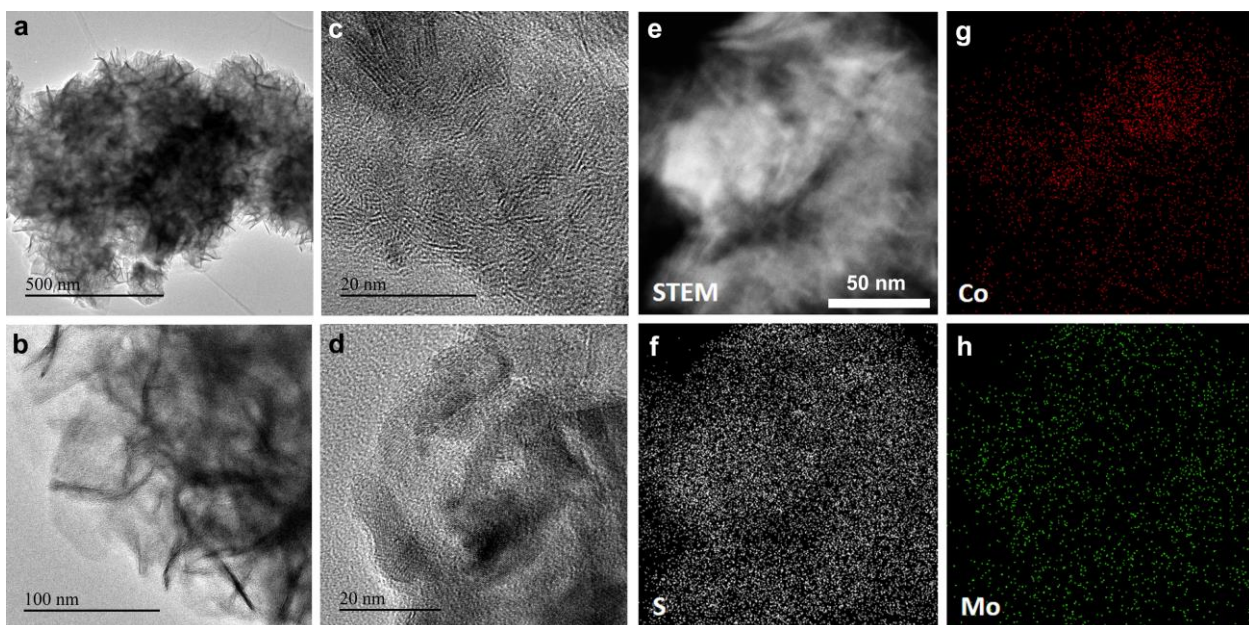


Figure 8. Morphological characterization of Co-Mo-S-0.39-180-R7 in two different areas. Low-magnification TEM images (a-b). HRTEM images (c-d). STEM-HAADF image (e). Elemental mapping of sulfur, cobalt and molybdenum (f-h)

Next, to get insights on the deactivation of this nanolayered Co-Mo-S catalyst, electron microscopy studies were carried out on the catalyst after the first and the seven run (Co-Mo-S-0.39-180-R1 and Co-Mo-S-0.39-180-R7, respectively). As shown Figure 7 and 8, while catalyst Co-Mo-S-0.39-180-R1 still displays the same morphology than the fresh catalyst (please, see also Figure 3e-f), a significant change can be noticed for catalyst Co-Mo-S-0.39-180-R7. In fact, its layered structure becomes less well defined being more deteriorated and with more disordered fringes. In addition, a detailed XEDS elemental mapping also reveals noticeable differences on its composition. Catalyst Co-Mo-S-0.39-180-R1 still shows a homogeneous distribution of cobalt on MoS₂ with Co/Mo weight ratios that range from 1:7 to 1:21 in concordance with the existing in the fresh catalyst. However, after the seven run these Co/Mo weight ratios become much higher (even up to 1:1) in some areas of catalyst Co-Mo-S-0.39-180-R7. These observations suggest that desorption of cobalt species from the MoS₂ backbone has occurred during successive reaction cycles, resulting in the formation of separated and agglomerated CoS₂, and thereby with the concomitant partial elimination of the Co-Mo-S like structures. In agreement with the Edge Decoration model proposed by Topsøe *et al.*, these Co-Mo-S structures, which consist of small MoS₂-like domains with cobalt promoter atoms adsorbed on MoS₂ edges, are proposed to be responsible for the promotion of the catalytic activity.^{26a-c,26e,26f} Therefore, its partial elimination should lead to a progressive dropping of the catalytic activity, as it has been observed during the successive reaction cycles.

SUMMARY

We have found that it is possible to carry out the hydrogenation of nitroarenes with high chemoselectivity in the presence of nanolayered molybdenum disulfide cobalt promoted materials (Co-Mo-S). With this type of catalysts, a wide range of nitroarenes have been hydrogenated to the corresponding anilines under relatively mild conditions. Notably, easily reducible functional moieties, such as double and triple bonds, aldehydes, ketones as well as carboxylic acid derivative groups, have been well tolerated allowing for obtaining the corresponding anilines in good to excellent yields. Interestingly, the partial hydrogenation of some dinitroarenes has also been successfully achieved in the presence of these nanolayered Co-Mo-S catalysts. In addition, through the preparation of paracetamol, the suitable use of these catalysts for the direct hydrogenative amidation of nitroarenes with carboxylic acids has been confirmed. In general, it constitutes a convenient catalytic protocol for the hydrogenation of nitroarenes since it makes use of an unsupported non-noble metal-based heterogeneous catalyst with a high number of active sites per unit volume, which offers compelling advantages for industrial applications. Comparing to their supported counterparts, these catalysts might allow for a more efficient reactor filling, thus providing the capability to process more feedstock. Active nanolayered Co-Mo-S catalysts have been prepared by a one-pot hydrothermal method by using cheap and abundant precursors. The effects of the catalyst preparation temperature and the cobalt content on the catalytic activity for the chemoselective hydrogenation of nitroarenes have been well established. It seems that the enhanced catalytic activity observed with the promoting effect of cobalt could be explained by the Edge Decoration model with the formation of Co-Mo-S like structures, and therefore their transformation lead to a variation in the hydrogenation activity.

EXPERIMENTAL SECTION

Preparation of Unsupported Catalysts

Unsupported Co-Mo-S catalysts were prepared by a one-pot hydrothermal synthesis. The catalyst preparation was carried out in a 130 mL Parr stirred reactor. Ammonium molybdate $[(\text{NH}_4)_6\text{Mo}_7\text{O}_{24}\cdot 4\text{H}_2\text{O}]$ (750 mg), elemental sulfur (283.4 mg) and cobalt acetate $[\text{Co}(\text{OAc})_2\cdot 4\text{H}_2\text{O}]$ were put in a stainless steel autoclave vessel. Then, distilled water (57 mL) and hydrazine monohydrate (64-65%, 5.5 mL) were added, the autoclave was enclosed tightly and purged twice with nitrogen as a leak testing. The mixture was heated and stirred until the desired internal temperature (150-210 °C) was reached (aprox. 60-90 min), and then maintain in static conditions at this temperature. After 22 h, the autoclave was naturally cooled to room temperature, and the generated gas was carefully released. The resulting nanolayered catalyst was recovered by filtration, washed with distilled water, ethanol and diethyl ether. Finally, the black solid catalyst was dried under vacuum for 1 h and stored under a nitrogen environment.

The composition of Co-Mo-S catalysts with different Co/(Mo+Co) mole ratio (0.17, 0.26, 0.39, 0.50) was change by using different amount of cobalt acetate in their preparation (92.6, 190.8, 295.6, 396.8 mg, respectively). The non-promoted MoS_2 catalyst was prepared by the same procedure as for the Co-Mo-S catalysts, but without addition of the cobalt precursor.³³

Catalysts Characterization

Powder X-ray diffraction (XRD) measurements were performed in a HTPhilips X'Pert MPD diffractometer equipped with a PW3050 goniometer using $\text{CuK}\alpha$ radiation and a multisampling handler.

Samples for electron microscopy studies were prepared by dropping a suspension of the nanolayered MoS₂-based catalysts in CH₂Cl₂ directly onto the holey-carbon-coated nickel grids. All measurements were performed in a JEOL 2100F microscope operating at 200 kV both in transmission (TEM) and scanning-transmission modes (STEM). STEM images were obtained using a high-angle annular dark-field detector (HAADF), which allows Z-contrast imaging.

The specific surface area and pore structures of the nanolayered MoS₂-based catalysts were determined by physisorption of N₂ by using the Brunauer–Emmett–Teller (BET) and Barrett–Joyner–Halenda (BJH) methods at 77 K and low relative pressure (P/P₀) of 0-0.25. The measurements were carried out in a Micromeritics ASAP 2420 gas adsorption analyzer, after degassing the samples at 473K for 24 h.

Hydrogenation of Nitroarenes

Catalytic hydrogenations were carried out in a 6 mL reinforced glass reactor equipped with a pressure control. The glass reactor containing a stirring bar was charged with the substrate (0.25 mmol), nanolayered Co-Mo-S catalyst (4.9 mg), dodecane (50 µL) as an internal standard and toluene (1.5 mL). Once sealed, reactor was purged by flushing five times with 10 bar of hydrogen, then pressurized to 11 bar and placed into aluminum block preheated at 150 °C. After reaction time, the reactor was cooled naturally to room temperature and the remaining gas was carefully released. Finally, the reaction mixture was diluted with ethyl acetate and analyzed by GC. All catalytic reactions were performed at least twice to ensure reproducibility. For the kinetic studies, magnetic stirring was switched off for 1 min to collect the catalyst on the bottom, and then 50 µL of the reaction mixture was taken out for GC analysis at different reaction times. To determine the isolated yields of the final amines, no internal standard was added. After

reaction, the mixture was diluted with ethyl acetate, filtered over celite to separate off the catalyst and taken to dryness under vacuum. It should be note that for some amines purification by silica gel chromatography was also carried out (see Supporting Information).

ASSOCIATED CONTENT

The Supporting Information is available free of charge via the Internet at <http://pubs.acs.org>.

Extended data about nanolayered Co-Mo-S catalysts characterization, optimization of reaction conditions, additional experimental results and procedures, characterization data of isolated products

AUTHOR INFORMATION

Corresponding Author

*acorma@itq.upv.es

Notes

The authors declare no competing financial interest.

ACKNOWLEDGMENT

The financial support of the European Union (FP7-NMP-2013-EU-Japan-604319-NOVACAM) is gratefully acknowledged. I.S. thanks Spanish MINECO for a “Formación Postdoctoral” fellowship. The authors also thank the Microscopy Service of Universitat Politècnica de València for kind help with TEM and STEM measurements.

REFERENCES

- (1) Wittcoff, H. A.; Reuben, B. G.; Plotkin, J. S. *in Industrial Organic Chemicals* 2nd ed.; Wiley-Interscience New York, 2004.

- (2) (a) Lawerencem, S. A. in *Amines: Synthesis, Properties and Applications* Cambridge University Cambridge, 2004. (b) Rappoport, Z. in *The Chemistry of Anilines, Part 1*; John Wiley & Sons Ltd Chichester (England) 2007.
- (3) (a) Downing, R. S.; Kunkeler, P. J.; vanBekkum, H. *Catal. Today* **1997**, *37*, 121-136. (b) Ono, N. in *The Nitro Group in Organic Synthesis*; Wiley-VCH: New York, 2001.
- (4) Kovar, F.; Armond, F. E. U.S. Patent 3,975,444, 1976.
- (5) Suchy, M.; Winternitz, P.; Zeller, M. World (WO) Patent 91/00278, 1991.
- (6) Butera, J.; Bagli, J. World (WO) Patent 91/09023, 1991.
- (7) Burawoy, A.; Critchley, J. P. *Tetrahedron* **1959**, *5*, 340-351.
- (8) (a) Blaser, H.-U.; Siegrist, U.; Steiner, H. in *Aromatic Nitro Compounds: Fine Chemicals Through Heterogeneous Catalysis*; Wiley-VCH: Weinheim, Germany, 2001. (b) Kadam, H. K.; Tilve, S. G. *RSC Adv.* **2015**, *5*, 83391-83407.
- (9) (a) Blaser, H.-U.; Steiner, H.; Studer, M. *Chemcatchem* **2009**, *1*, 210-221. (b) Serna, P.; Corma, A. *Acs Catal.* **2015**, *5*, 7114-7121.
- (10) Siegrist, U.; Baumeister, P.; Blaser, H.-U.; Studer, M. *Chem. Ind. (Dekker)* **1998**, *75*, 207-219.
- (11) (a) Corma, A.; Serna, P. *Science* **2006**, *313*, 332-334. (b) Corma, A.; Serna, P. *Nat. Protoc.* **2007**, *1*, 2590-2595. (c) Boronat, M.; Concepción, P.; Corma, A.; González, S.; Illas, F.; Serna, P. *J. Am. Chem. Soc.* **2007**, *129*, 16230-16237. (d) Corma, A.; Concepción, P.; Serna, P. *Angew. Chem. Int. Ed.* **2007**, *46*, 7266-7269. (e) Serna, P.; Concepción, P.; Corma, A. *J. Catal.* **2009**, *265*, 19-25. (f) Serna, P.; Boronat, M.; Corma, A. *Top. Catal.* **2011**, *54*, 439-446.
- (12) Corma, A.; Serna, P.; Concepcion, P.; Calvino, J. J. *J. Am. Chem. Soc.* **2008**, *130*, 8748-8753.
- (13) (a) Shimizu, K.-i.; Miyamoto, Y.; Kawasaki, T.; Tanji, T.; Tai, Y.; Satsuma, A. *J. Phys. Chem. C* **2009**, *113*, 17803-17810. (b) Matsushima, Y.; Nishiyabu, R.; Takanashi, N.; Haruta, M.; Kimura, H.; Kubo, Y. *J. Mater. Chem.* **2012**, *22*, 24124-24131. (c) Makosch, M.; Lin, W.-I.; Bumbalek, V.; Sa, J.; Medlin, J. W.; Hungerbuehler, K.; van Bokhoven, J. A. *Acs Catal.* **2012**, *2*, 2079-2081. (d) Wei, H.; Liu, X.; Wang, A.; Zhang, L.; Qiao, B.; Yang, X.; Huang, Y.; Miao, S.; Liu, J.; Zhang, T. *Nat. Commun.* **2014**, *5*, 5634.
- (14) (a) Shimizu, K.-i.; Miyamoto, Y.; Satsuma, A. *J. Catal.* **2010**, *270*, 86-94. (b) Mitsudome, T.; Mikami, Y.; Matoba, M.; Mizugaki, T.; Jitsukawa, K.; Kaneda, K. *Angew. Chem. Int. Ed.* **2012**, *51*, 136-139.
- (15) Furukawa, S.; Yoshida, Y.; Komatsu, T. *Acs Catal.* **2014**, *4*, 1441-1450.
- (16) (a) Westerhaus, F. A.; Jagadeesh, R. V.; Wienhoefer, G.; Pohl, M.-M.; Radnik, J.; Surkus, A.-E.; Rabeah, J.; Junge, K.; Junge, H.; Nielsen, M.; Brueckner, A.; Beller, M. *Nat. Chem.* **2013**, *5*, 537-543. (b) Jagadeesh, R. V.; Surkus, A.-E.; Junge, H.; Pohl, M.-M.; Radnik, J.; Rabeah, J.; Huan, H.; Schuenemann, V.; Brueckner, A.; Beller, M. *Science* **2013**, *342*, 1073-1076. (c) Jagadeesh, R. V.; Stemmler, T.; Surkus, A.-E.; Bauer, M.; Pohl, M.-M.; Radnik, J.; Junge, K.; Junge, H.; Brueckner, A.; Beller, M. *Nat. Protoc.* **2015**, *10*, 916-926. (d) Jagadeesh, R. V.; Stemmler, T.; Surkus, A.-E.; Bauer, M.; Pohl, M.-M.; Radnik, J.; Junge, K.; Junge, H.; Brueckner, A.; Beller, M. *Nat. Protoc.* **2016**, *11*, 192-192. (e) Jagadeesh, R. V.; Stemmler, T.; Surkus, A.-E.; Junge, H.; Junge, K.; Beller, M. *Nat. Protoc.* **2015**, *10*, 548-557.
- (17) Formenti, D.; Topf, C.; Junge, K.; Ragaini, F.; Beller, M. *Catal. Sci. Technol.* **2016**, *6*, 4473-4477.

- (18) (a) Wei, Z.; Wang, J.; Mao, S.; Su, D.; Jin, H.; Wang, Y.; Xu, F.; Li, H.; Wang, Y. *Acs Catal.* **2015**, *5*, 4783-4789. (b) Schwob, T.; Kempe, R. *Angew. Chem. Int. Ed.* **2016**, *55*, 15175-15179. (c) Wang, X.; Li, Y. *J. Mol. Catal. A: Chem.* **2016**, *420*, 56-65.
- (19) (a) Liu, L.; Concepción, P.; Corma, A. *J. Catal.* **2016**, *340*, 1-9. (b) For other example mediated by a nitrogen-free Co/CoO@C catalyst under harsher reaction conditions, see: Chen, B.; Li, F.; Huang, Z.; Yuan, G. *ChemCatChem* **2016**, *8*, 1132-1138.
- (20) (a) Casewit, C. J.; Coons, D. E.; Wright, L. L.; Miller, W. K.; DuBois, M. R. *Organometallics* **1986**, *5*, 951-955. (b) Sorribes, I.; Wienhoefer, G.; Vicent, C.; Junge, K.; Llusar, R.; Beller, M. *Angew. Chem. Int. Ed.* **2012**, *51*, 7794-7798. (c) Pedrajas, E.; Sorribes, I.; Junge, K.; Beller, M.; Llusar, R. *Chemcatchem* **2015**, *7*, 2675-2681. (d) Pedrajas, E.; Sorribes, I.; Gushchin, A. L.; Laricheva, Y. A.; Junge, K.; Beller, M.; Llusar, R. *ChemCatChem* **2017**, *9*, in press, <http://dx.doi.org/10.1002/cctc.201601496>.
- (21) (a) Huang, L.; Luo, P.; Xiong, M.; Chen, R.; Wang, Y.; Xing, W.; Huang, J. *Chin. J. Chem.* **2013**, *31*, 987-991. (b) Zhang, C.; Zhang, Z.; Wang, X.; Li, M.; Lu, J.; Si, R.; Wang, F. *Appl. Catal., A* **2016**, *525*, 85-93.
- (22) Srivastava, S. K.; Avasthi, B. N. *J. Mater. Sci.* **1993**, *28*, 5032-5035.
- (23) Sun, D.-Y.; Lin, B.-Z.; Xu, B.-H.; He, L.-W.; Ding, C.; Chen, Y.-L. *J. Porous Mater.* **2008**, *15*, 245-251.
- (24) Kamiguchi, S.; Arai, K.; Okumura, K.; Iida, H.; Nagashima, S.; Chihara, T. *Appl. Catal., A* **2015**, *505*, 417-421.
- (25) (a) Topsøe, H.; Clausen, B. S.; Massoth, F. E.; (Eds. Anderson, J. R.; Moudart, M. *in Hydrotreating Catalysis-Science and Technology*; Springer-Verlag: Berlin, 1996; Vol. 11. (b) Brorson, M.; Carlsson, A.; Topsoe, H. *Catal. Today* **2007**, *123*, 31-36. (c) Jaramillo, T. F.; Jorgensen, K. P.; Bonde, J.; Nielsen, J. H.; Horch, S.; Chorkendorff, I. *Science* **2007**, *317*, 100-102. (d) Wang, S.; Zhang, J.; He, D.; Zhang, Y.; Wang, L.; Xu, H.; Wen, X.; Ge, H.; Zhao, Y. *J. Phys. Chem. Solids* **2014**, *75*, 100-104.
- (26) (a) Topsoe, H.; Clausen, B. S.; Candia, R.; Wivel, C.; Morup, S. *J. Catal.* **1981**, *68*, 433-452. (b) Wivel, C.; Candia, R.; Clausen, B. S.; Morup, S.; Topsoe, H. *J. Catal.* **1981**, *68*, 453-463. (c) Clausen, B. S.; Topsoe, H.; Candia, R.; Villadsen, J.; Lengeler, B.; Alsniesen, J.; Christensen, F. *J. Phys. Chem.* **1981**, *85*, 3868-3872. (d) Breyse, M.; Bennett, B. A.; Chadwick, D.; Vrinat, M. *Bull. Soc. Chim. Belg.* **1981**, *90*, 1271-1277. (e) Topsoe, N. Y.; Topsoe, H. *J. Catal.* **1983**, *84*, 386-401. (f) Kasztelan, S.; Toulhoat, H.; Grimblot, J.; Bonnelle, J. P. *Appl. Catal.* **1984**, *13*, 127-159. (g) Topsøe, H.; Clausen, B. S. *Appl. Catal.* **1986**, *25*, 273-293. (h) Daage, M.; Chianelli, R. R. *J. Catal.* **1994**, *149*, 414-427. (i) Byskov, L. S.; Nørskov, J. K.; Clausen, B. S.; Topsøe, H. *J. Catal.* **1999**, *187*, 109-122. (j) Schweiger, H.; Raybaud, P.; Toulhoat, H. *J. Catal.* **2002**, *212*, 33-38. (k) Lauritsen, J. V.; Bollinger, M. V.; Lægsgaard, E.; Jacobsen, K. W.; Nørskov, J. K.; Clausen, B. S.; Topsøe, H.; Besenbacher, F. *J. Catal.* **2004**, *221*, 510-522. (l) Topsoe, H. *Appl. Catal., A* **2007**, *322*, 3-8. (m) Lauritsen, J. V.; Kibsgaard, J.; Olesen, G. H.; Moses, P. G.; Hinnemann, B.; Helveg, S.; Nørskov, J. K.; Clausen, B. S.; Topsøe, H.; Lægsgaard, E.; Besenbacher, F. *J. Catal.* **2007**, *249*, 220-233. (n) Berhault, G.; Perez De la Rosa, M.; Mehta, A.; Yácaman, M. J.; Chianelli, R. R. *Appl. Catal., A* **2008**, *345*, 80-88. (o) Besenbacher, F.; Brorson, M.; Clausen, B. S.; Helveg, S.; Hinnemann, B.; Kibsgaard, J.; Lauritsen, J. V.; Moses, P. G.; Nørskov, J. K.; Topsøe, H. *Catal. Today* **2008**, *130*, 86-96. (p) Gandubert, A. D.; Krebs, E.; Legens, C.; Costa, D.; Guillaume, D.; Raybaud, P. *Catal. Today* **2008**, *130*, 149-159. (q) Krebs, E.; Silvi, B.; Raybaud, P.

- Catal. Today* **2008**, *130*, 160-169. (r) Kibsgaard, J.; Tuxen, A.; Knudsen, K. G.; Brorson, M.; Topsøe, H.; Lægsgaard, E.; Lauritsen, J. V.; Besenbacher, F. *J. Catal.* **2010**, *272*, 195-203. (s) Zhu, Y.; Ramasse, Q. M.; Brorson, M.; Moses, P. G.; Hansen, L. P.; Kisielowski, C. F.; Helveg, S. *Angew. Chem. Int. Ed.* **2014**, *53*, 10723-10727.
- (27) Byskov, L. S.; Hammer, B.; Norskov, J. K.; Clausen, B. S.; Topsoe, H. *Catal. Lett.* **1997**, *47*, 177-182.
- (28) (a) Lauritsen, J. V.; Nyberg, M.; Norskov, J. K.; Clausen, B. S.; Topsoe, H.; Laegsgaard, E.; Besenbacher, F. *J. Catal.* **2004**, *224*, 94-106. (b) Berit, H.; Poul Georg, M.; Jens, K. *N. J. Phys.: Condens. Matter* **2008**, *20*, 064236. (c) Temel, B.; Tuxen, A. K.; Kibsgaard, J.; Topsøe, N.-Y.; Hinnemann, B.; Knudsen, K. G.; Topsøe, H.; Lauritsen, J. V.; Besenbacher, F. *J. Catal.* **2010**, *271*, 280-289. (d) Rangarajan, S.; Mavrikakis, M. *Acc Catal.* **2016**, *6*, 2904-2917.
- (29) (a) Soled, S. L.; Miseo, S.; Krycak, R.; Vroman, H.; Ho, T. C.; Riley, K. U. S. Patent 6,299,760 to Exxonmobil, 2001. (b) Plantenga, F. L.; Cerfontain, R.; Eijsbouts, S.; van Houtert, F.; Anderson, G. H.; Miseo, S.; Soled, S.; Riley, K.; Fujita, K.; Inoue, Y. In *Stud. Surf. Sci. Catal.*; Anpo, M., Onaka, M., Yamashita, H., Eds.; Elsevier: 2003; Vol. Volume 145, p 407-410.
- (30) (a) Yoosuk, B.; Tumnantong, D.; Prasassarakich, P. *Chem. Eng. Sci.* **2012**, *79*, 1-7. (b) Eijsbouts, S.; Mayo, S. W.; Fujita, K. *Appl. Catal., A* **2007**, *322*, 58-66.
- (31) Liu, N.; Wang, X.; Xu, W.; Guo, D.; Tang, J.; Zhang, B. *Prog. Chem.* **2013**, *25*, 726-734.
- (32) (a) Yoosuk, B.; Song, C.; Kim, J. H.; Ngamcharussrivichai, C.; Prasassarakich, P. *Catal. Today* **2010**, *149*, 52-61. (b) Yoosuk, B.; Tumnantong, D.; Prasassarakich, P. *Fuel* **2012**, *91*, 246-252. (c) Wang, W.; Zhang, K.; Li, L.; Wu, K.; Liu, P.; Yang, Y. *Ind. Eng. Chem. Res.* **2014**, *53*, 19001-19009. (d) Itthibenchapong, V.; Ratanatawanate, C.; Oura, M.; Faungnawakij, K. *Catal. Commun.* **2015**, *68*, 31-35. (e) Wang, W.; Li, L.; Wu, K.; Zhu, G.; Tan, S.; Li, W.; Yang, Y. *RSC Adv.* **2015**, *5*, 61799-61807. (f) Wang, W.; Li, L.; Wu, K.; Zhang, K.; Jie, J.; Yang, Y. *Appl. Catal., A* **2015**, *495*, 8-16. (g) Wang, W.; Li, L.; Tan, S.; Wu, K.; Zhu, G.; Liu, Y.; Xu, Y.; Yang, Y. *Fuel* **2016**, *179*, 1-9. (h) Wang, W.; Li, L.; Wu, K.; Zhu, G.; Tan, S.; Liua, Y.; Yang, Y. *RSC Adv.* **2016**, *6*, 31265-31271. (i) Wang, W.; Wu, K.; Li, L.; Tan, S.; Zhu, G.; Li, W.; He, Z.; Yang, Y. *Catal. Commun.* **2016**, *74*, 60-64. (j) Wang, W.; Zhu, G.; Li, L.; Tan, S.; Wu, K.; Zhang, X.; Yang, Y. *Fuel* **2016**, *174*, 1-8.
- (33) (a) Peng, Y. Y.; Meng, Z. Y.; Zhong, C.; Lu, J.; Yu, W. C.; Jia, Y. B.; Qian, Y. T. *Chem. Lett.* **2001**, 772-773. (b) Peng, Y. Y.; Meng, Z. Y.; Zhong, C.; Lu, J.; Yu, W. C.; Yang, Z. P.; Qian, Y. T. *J. Solid State Chem.* **2001**, *159*, 170-173.
- (34) (a) Park, S.-K.; Yu, S.-H.; Woo, S.; Ha, J.; Shin, J.; Sung, Y.-E.; Piao, Y. *CrystEngComm* **2012**, *14*, 8323-8325. (b) Wang, Z.; Chen, T.; Chen, W.; Chang, K.; Ma, L.; Huang, G.; Chen, D.; Lee, J. Y. *J. Mater. Chem. A* **2013**, *1*, 2202-2210.
- (35) Yi, Y.; Zhang, B.; Jin, X.; Wang, L.; Williams, C. T.; Xiong, G.; Su, D.; Liang, C. *J. Mol. Catal. A: Chem.* **2011**, *351*, 120-127.
- (36) (a) Delmon, B. *C. R. Hebd. Seances Acad. Sci. Serie C* **1979**, *289*, 173-176. (b) Delmon, B. *Bull. Soc. Chim. Belg.* **1979**, *88*, 979-987. (c) Weng, L. T.; Delmon, B. *Appl. Catal., A* **1992**, *81*, 141-213. (d) Stumbo, A. M.; Grange, P.; Delmon, B. *Catal. Lett.* **1995**, *31*, 173-182. (e) Delmon, B.; Froment, G. F. *Catal. Rev. Sci. Eng.* **1996**, *38*, 69-100. (f) Stumbo, M.; Grange, P.; Delmon, B.; (Eds. Li, C.; Xin, Q. in *Spillover and Migration of Surface Species on Catalysts*; Elsevier Science B.V., 1997.

- (37) Li, X.-G.; Huang, M.-R.; Duan, W.; Yang, Y.-L. *Chem. Rev.* **2002**, *102*, 2925-3030.
- (38) Haber, F. *Z. Elektrochem.* **1898**, *22*, 506.
- (39) Joncour, R.; Duguet, N.; Metay, E.; Ferreira, A.; Lemaire, M. *Green Chem.* **2014**, *16*, 2997-3002.
- (40) Bhattacharya, A.; Purohit, V. C.; Suarez, V.; Tichkule, R.; Parmer, G.; Rinaldi, F. *Tetrahedron Lett.* **2006**, *47*, 1861-1864.
- (41) Li, M.; Hu, L.; Cao, X.; Hong, H.; Lu, J.; Gu, H. *Chem. Eur. J.* **2011**, *17*, 2763-2768.
- (42) Kumar, V.; Kumar, M.; Sharma, S.; Kumar, N. *RSC Adv.* **2014**, *4*, 11826-11830.

TABLE OF CONTENTS ARTWORK

